Ocean Engineering 286 (2023) 115553

Contents lists available at ScienceDirect

Ocean Engineering

journal homepage: www.elsevier.com/locate/oceaneng

Single neural network-based asymptotic adaptive control for an autonomous underwater vehicle with uncertain dynamics

Yuxi Zhang, Jiapeng Liu *, Jinpeng Yu, Dongxiao Liu

School of Automation, Qingdao University, Qingdao 250061, 266071, China

ARTICLE INFO

Keywords:
Autonomous underwater vehicle
Neural network
Asymptotic control
Uncertainty problem
Adaptive control

ABSTRACT

This paper focuses on the adaptive asymptotic tracking control problem for an autonomous underwater vehicle (AUV) with un-modeled dynamics and unknown input saturation by combining the backstepping control strategy and the neural network (NN) method. In our controller, a novel single neural network-based backstepping control method is proposed to address the uncertain problem, and the input saturation issue is overcome in virtue of a hyperbolic tangent function. The approximation error of the neural network is also compensated by a new adaptive mechanism in order to achieve the zero-error regulation. Furthermore, the nonlinear transformation is incorporated into the backstepping-based framework to improve the AUV performance. And then, the performance analysis illustrates that the designed controller can realize the asymptotic stability of the AUV system. Finally, the effectiveness of our control strategy is validated through simulation results.

1. Introduction

AUVs have exhibited significant benefits in the exploration of marine resources and the monitoring of aquatic environments (Fang et al., 2022). As one of the significant topics in the field of AUV motion control, the uncertainty problem caused by model mismatch and unknown external disturbances has attracted significant attentions. The ambition to obtain a high-precision trajectory tracking controller for AUVs leads to the use of neural network techniques, and lots of control strategies have been developed over recent years (Elhaki and Shojaei, 2018). In Che and Yu (2020), the adaptive dynamic programming control strategy with neural network estimators is proposed for AUVs in the presence of rudders faults and disturbances. In Zhang et al. (2021), the approach-angle-based tracking control method is proposed for the three-dimensional underactuated autonomous underwater vehicle with unknown actuator saturation and environmental disturbance based on the indirect adaptive fuzzy method. In Zhang et al. (2020), the neural network-based adaptive control method is given for the underactuated AUV with saturation and unknown dynamics.

The above studies clearly indicate that the uncertain issue in the AUVs can be solved in virtue of the neural network approximators. However, it is still a challenging task to design an accurate tracking trajectory control method for the uncertain AUV by using network based control framework. In practice, the architecture of neural networks, such as node numbers and activation functions, is pre-defined based on engineering experiences and AUV system features. And then, the weight vectors of neural networks are dynamically updated by employing error-driven adaptive laws. Thus, the neural network with the adaptive weights would only approximate the unknown function in the AUV systems with a limited precision (Ding et al., 2022; Mohammadi et al., 2022; Wang et al., 2019). It is almost impossible to completely eliminate the approximation error even though employing more complex neural networks, such as the convolutional neural network (CNN). Furthermore, the σ-modified adaptive laws are employed in those results to ensure the boundedness of the adaptive weights. The updating weight may converge to the neighborhood of the zero, not to the neighborhood of the ideal point, which may lead to a relatively large tracking error for the existing adaptive NN controllers. Hence, the asymptotic convergence of tracking errors cannot always be guaranteed under above-mentioned adaptive neural control strategies. As the authors know, limited results have been reported on the neural network-based asymptotic adaptive control problem for the AUVs with model uncertainties.

On the other hand, the huge difference in system dynamics over different degrees of freedom also increases the design difficulty for the AUV controller. An independent adaptive neural network module should be used for each subsystem in the AUVs to improve the control performance. For example, a standard adaptive neural network-based controller for three degrees of freedom AUVs requires at least three neural networks and three adaptive laws. Considering the limited

* Corresponding author.
E-mail addresses: ljpqdu1990@qdu.edu.cn (J. Liu), yjp1109@qdu.edu.cn (J. Yu).

https://doi.org/10.1016/j.oceaneng.2023.115553
Received 23 May 2023; Received in revised form 3 July 2023; Accepted 2 August 2023

calculation resource in the AUV control system, the solution process of neural networks and adaptive weights is time-consuming, which may influence the control performance. It should be noted that the over-parameterization problem of the adaptive neural backstepping control strategies has received increasing attentions in recent years. In Yu et al. (2020), a novel adaptive neural control method that only contains one adaptive law is proposed for high-order uncertain systems through Young's Inequality and backstepping scheme. And in Liu et al. (2022), the research on the simplification problem of the event-triggered adaptive neural controller is also carried out. However, decreasing the number of neural networks is still a critical issue in the real-time implementation of the above-mentioned adaptive neural network controllers. Thus, the research on reducing the calculation load of the adaptive neural controller and eliminating the effect of approximation errors is meaningful in the field of AUVs' motion control. And it is the main motivation of our paper.

In this paper, a novel asymptotic adaptive neural backstepping-based control method is developed for the AUV with model uncertainty and unknown input saturation. The tracking performance is improved by incorporating a new nonlinear transformation into the backstepping technique. The asymptotic stability is also proven on the basis of Barbalat's Lemma. And, our main contributions are listed as follows.

(1) Unlike existing adaptive control methods (Zong et al., 2021; Shojaei, 2022; Li et al., 2019), our algorithm guarantees the asymptotic convergence of tracking errors by introducing a new adaptive law to compensate the approximate error.

(2) Compared with adaptive neural approaches that use multi-neural network approximators (Zhao et al., 2018; Wang et al., 2019; Ding et al., 2022), only one single neural network and two adaptive laws are required in our strategy, which reduces the calculation burden of the AUV control system.

(3) The virtual stabilizing functions are re-constructed by using a new nonlinear transformation to improve the tracking performance, which implies that the tracking errors are located in the pre-defined region.

After the introduction in Sections 1, 2 gives the mathematical model for the AUV. Section 3 develops the adaptive neural-based asymptotic control method. Section 4 presents the performance analysis and Section 5 shows simulation results. Section 6 summarizes the study and provides our conclusion.

2. Preliminaries and problem formulation

The mathematical dynamic model for a three degree of freedom AUV (Fossen, 2002) is

$$\dot{x} = v_x \cos\xi - v_y \sin\xi \tag{1}$$

$$\dot{y} = v_x \sin\xi + v_y \cos\xi \tag{2}$$

$$\dot{\xi} = v_\xi \tag{3}$$

$$\dot{v}_x = \frac{M_{\dot{v}_y}}{M_{\dot{v}_x}} v_y v_\xi - \frac{X_{v_x}}{M_{\dot{v}_x}} v_x - \frac{D_{v_x}}{M_{\dot{v}_x}} v_x |v_x| + \frac{\tau_1}{M_{\dot{v}_x}} \tag{4}$$

$$\dot{v}_y = -\frac{M_{\dot{v}_x}}{M_{\dot{v}_y}} v_x v_\xi - \frac{Y_{v_y}}{M_{\dot{v}_y}} v_y - \frac{D_{v_y}}{M_{\dot{v}_y}} v_y |v_y| + \frac{\tau_2}{M_{\dot{v}_y}} \tag{5}$$

$$\dot{v}_\xi = \frac{M_{\dot{v}_x} - M_{\dot{v}_y}}{M_{\dot{v}_\xi}} v_x v_y - \frac{N_{v_\xi}}{M_{\dot{v}_\xi}} v_\xi - \frac{D_{v_\xi}}{M_{\dot{v}_\xi}} v_\xi |v_\xi| + \frac{\tau_3}{M_{\dot{v}_\xi}} \tag{6}$$

where x, y and ξ are the surge, sway and yaw for the AUV, respectively. And v_x, v_y and v_ξ indicate the AUV speeds in different directions, as shown in Fig. 1. Besides, $M_{\dot{v}_x}$, $M_{\dot{v}_y}$ and $M_{\dot{v}_\xi}$ are inertia tensor coefficients, m is mass of AUVs, I_z is the moment of inertia about the vertical direction, $X_{\dot{v}_x}$, $Y_{\dot{v}_y}$ and $N_{\dot{v}_\xi}$ denote second order hydrodynamic damping coefficients. X_{v_x}, Y_{v_y}, N_{v_ξ}, D_{v_x}, D_{v_y} and D_{v_ξ} indicate first order hydrodynamic damping coefficients. Moreover, τ_1 is surge force, τ_2 is sway force and τ_3 is yaw moment, which are described as (von Ellenrieder, 2019)

$$\tau_i \approx u_M \tanh\left(\frac{u_i}{u_M}\right) \tag{7}$$

where $i = 1, 2, 3$, u_i are actual control laws, u_M is a unknown saturation parameter. In order to overcome the uncertain nonlinear problem caused by $\tanh(.)$, τ_i can also be expressed as (Wang et al., 2014),

$$\tau_i = \tau_{i\mu} u_i \tag{8}$$

where $\tau_{i\mu} = 4/\left(e^{u_i/u_M} + e^{-u_i/u_M}\right)^2|_{u_i=u_{i\mu}}$, $u_{i\mu} = \mu u_i$ and the value $\mu \in (0, 1)$ is unknown.

It is noteworthy that all the system parameters m, I_z, $X_{\dot{v}_x}$, $Y_{\dot{v}_y}$, $N_{\dot{v}_\xi}$, X_{v_x}, Y_{v_y}, N_{v_ξ}, D_{v_x}, D_{v_y} and D_{v_ξ} are completely unknown. Thus, we adopt the radial basis function (RBF) neural network to deal with the un-modeled dynamics problem in AUV systems (Shang et al., 2018). The RBF neural network is:

$$f(\sigma) = W^T \Lambda(\sigma) \tag{9}$$

where $W = [W_1 \dots W_N]^T$ is weight vector, N denotes neural network node number, $\sigma = [x_1, \dots, x_N]^T \in \Gamma_\sigma \subset R^N$ means is input vector. $\Lambda(\sigma) = [\lambda_1(\sigma) \dots \lambda_N(\sigma)]^T$ is the basis function vector, and the function $\lambda_q(\sigma)$ is set to the following Gaussian function

$$\lambda_q(\sigma) = \exp\left[\frac{-(\sigma - H_q)^T(\sigma - H_q)}{\mu^2}\right] \tag{10}$$

where $q = 1, \dots, N$, μ means the width in the Gaussian function, and $H_q = [h_{q1}, \dots h_{qN}]^T$ is the center of the receptive field.

Lemma 1 (*Wang et al., 2013*). *Consider any continuous nonlinear function $f_i(\sigma_i)$ over a compact set $\Gamma_\sigma \subset R^n$, the following equation holds*

$$f_i(\sigma_i) = W_i^{*T} \Lambda_i(\sigma_i) + \delta_i(\sigma_i), \forall \sigma_i \in \Gamma_\sigma \subset R^n \tag{11}$$

where $\delta_i(\sigma_i)$ is the approximation error that satisfies $|\delta_i(\sigma_i)| < \varepsilon_i$ with an unknown constant ε_i. And the ideal weight vector W_i^* is

$$W_i^* = \arg\min_{W_i \in \bar{R}^N} \left\{ \sup_{\sigma_i \in \Gamma_\sigma} \left| f_i(\sigma_i) - W_i^T \Lambda_i(\sigma_i) \right| \right\} \tag{12}$$

Lemma 2 (*Yu et al., 2023*). *Let $\Lambda(\sigma_{s_1}) = \left[\lambda_1(\sigma_{s_1}), \dots, \lambda_N(\sigma_{s_1})\right]^T$ and $\Lambda(\sigma_{s_2}) = \left[\lambda_1(\sigma_{s_2}), \dots, \lambda_N(\sigma_{s_2})\right]^T$ be the basic function vectors in the RBF NN with $\sigma_{s_1} = \left[x_1, x_2, \dots, x_{s_1}\right]^T$ and $\sigma_{s_2} = \left[x_1, x_2, \dots, x_{s_2}\right]^T$. If s_1 and s_2 satisfy $s_1 < s_2$, then the following inequality holds:*

$$\left\|\Lambda(\sigma_{s_2})\right\|^2 \le \left\|\Lambda(\sigma_{s_1})\right\|^2 \tag{13}$$

Lemma 3 (*Zuo and Wang, 2014*). *Consider any $a \in R$ and $b > 0$, one has*

$$0 \le |a| - \frac{a^2}{\sqrt{a^2 + b^2}} < b. \tag{14}$$

Assumption 1 (*Fossen, 2002; Fischer et al., 2014*). The yaw angle falls within a known set $|\xi| < \pi/2$ to avoid the problem of singularity.

Assumption 2 (*Yu et al., 2020; von Ellenrieder, 2019*). The reference signals x_d, y_d, ξ_d and $\dot{x}_d$, $\dot{y}_d$, $\dot{\xi}_d$ are bound, smooth, and continuous.

Our control objective is to design the adaptive neural controller for the AUV (1)–(6) to make the AUV along the desired trajectory and ensure the asymptotic stability considering the unknown dynamics and input saturation. In order to develop a state-feedback backstepping-based control strategy, all the state variables in the system (1)–(6) are assumed to be obtained accurately.

3. Single neural network-based backstepping control scheme

3.1. Nonlinear transformation

Firstly, the tracking errors are $e_{11} = x - x_d$, $e_{21} = y - y_d$, $e_{31} = \xi - \xi_d$, $e_{12} = \nu_x - \alpha_1$, $e_{22} = \nu_y - \alpha_2$ and $e_{32} = \nu_\xi - \alpha_3$, where x_d, y_d, ξ_d are the desired trajectories, and α_1, α_2 and α_3 are virtual stabilizing laws. And then, introduce the coordinate transformation (Choi and Yoo, 2019) as

$$Q_{ij} = \frac{e_{ij}}{k} \tag{15}$$

$$\Phi\left(Q_{ij}\right) = \ln\left(\theta_u\theta_s + \theta_u Q_{ij}\right) - \ln\left(\theta_u\theta_s - \theta_s Q_{ij}\right) \tag{16}$$

where $j = 1, 2$, $i = 1, 2, 3$, $k_0 > 0$, $k_\infty > 0$, $\iota > 0$, $\theta_s > 0$, $\theta_u \le 1$, and $k(t) = \left(k_0 - k_\infty\right)e^{-\iota t} + k_\infty$. Thus, for $\forall t > 0$ and $-\theta_s k_0 < e_{ij}(0) < \theta_u k_0$, we have

$$-\theta_s k(t) < e_{ij}(t) < \theta_u k(t) \tag{17}$$

3.2. Control design

Step 1: For subsystem (1), the tracking error z_{i1} is

$$z_{i1} = \ln\left(\theta_u\theta_s + \theta_u Q_{i1}\right) - \ln\left(\theta_u\theta_s - \theta_s Q_{i1}\right). \tag{18}$$

$$Q_{i1} = \frac{e_{i1}}{k} \tag{19}$$

Hence, the Lyapunov function V_1 is chosen as

$$V_1 = \frac{1}{2}z_{11}^2 + \frac{1}{2}z_{21}^2 + \frac{1}{2}z_{31}^2 \tag{20}$$

Taking the derivative of V_1, we have

$$\begin{aligned}\dot{V}_1 &= z_{11}\phi_{11}\left(\nu_x\cos\xi - \nu_y\sin\xi - \dot{x}_d - e_{11}\dot{k}/k\right)\\ &+ z_{21}\phi_{21}\left(\nu_x\sin\xi + \nu_y\cos\xi - \dot{y}_d - e_{21}\dot{k}/k\right)\\ &+ z_{31}\phi_{31}\left(\nu_\xi - \dot{\xi}_d - e_{31}\dot{k}/k\right)\\ &= z_{11}\phi_{11}\left(\left(e_{12}+\alpha_1\right)\cos\xi - \left(e_{22}+\alpha_2\right)\sin\xi - \dot{x}_d - e_{11}\dot{k}/k\right)\\ &+ z_{21}\phi_{21}\left(\left(e_{12}+\alpha_1\right)\sin\xi + \left(e_{22}+\alpha_2\right)\cos\xi - \dot{y}_d - e_{21}\dot{k}/k\right)\\ &+ z_{31}\phi_{31}\left(e_{32}+\alpha_3 - \dot{\xi}_d - e_{31}\dot{k}/k\right)\end{aligned} \tag{21}$$

where $\phi_{ij} = 1/\left(e_{ij} + \theta_s k\right) - 1/\left(e_{ij} - \theta_u k\right) > 0$.

Design the virtual control laws α_i as

$$\alpha_1 = \left(-k_1 z_{11} + \dot{x}_d + e_{11}\dot{k}/k\right)\cos\xi + \left(-k_1 z_{21} + \dot{y}_d + e_{21}\dot{k}/k\right)\sin\xi \tag{22}$$

$$\alpha_2 = -\left(-k_1 z_{11} + \dot{x}_d + e_{11}\dot{k}/k\right)\sin\xi + \left(-k_1 z_{21} + \dot{y}_d + e_{21}\dot{k}/k\right)\cos\xi \tag{23}$$

$$\alpha_3 = -k_1 z_{31} + \dot{\xi}_d + e_{31}\dot{k}/k \tag{24}$$

where k_1 is a positive constant. Substituting Eqs. (22)–(24) into Eqs. (21), results into

$$\begin{aligned}\dot{V}_1 &= z_{11}\phi_{11}(-k_1 z_{11} + e_{12}\cos\xi - e_{22}\sin\xi)\\ &+ z_{21}\phi_{21}(-k_1 z_{21} + e_{12}\sin\xi + e_{22}\cos\xi) + z_{31}\phi_{31}(-k_1 z_{31} + e_{32})\\ &= -k_1 z_{11}^2\phi_{11} - k_1 z_{21}^2\phi_{21} - k_1 z_{31}^2\phi_{31} + (z_{11}\phi_{11}\cos\xi + z_{21}\phi_{21}\sin\xi)e_{12}\\ &+ (-z_{11}\phi_{11}\sin\xi + z_{21}\phi_{21}\cos\xi)e_{22} + z_{31}\phi_{31}e_{32}\end{aligned} \tag{25}$$

Step 2: Introduce the tracking error z_{i2} as

$$z_{i2} = \ln\left(\theta_u\theta_s + \theta_u Q_{i2}\right) - \ln\left(\theta_u\theta_s - \theta_s Q_{i2}\right) \tag{26}$$

$$Q_{i2} = \frac{e_{i2}}{k} \tag{27}$$

Choose the Lyapunov function V_2 as

$$V_2 = V_1 + \frac{1}{2\underline{E_1}}z_{12}^2 + \frac{1}{2\underline{E_2}}z_{22}^2 + \frac{1}{2\underline{E_3}}z_{32}^2 + \frac{1}{2\gamma}\tilde{A}^2 + \frac{1}{2r}\tilde{B}^2 \tag{28}$$

where γ and r are known positive constants, $\hat{A}$ is the estimated value of A, $\hat{B}$ is the estimated value of B, $\tilde{A} = A - \hat{A}$, $\tilde{B} = B - \hat{B}$. In addition, $\underline{E_i}$ is the minimum value of E_i, and the definitions of A, B and E_i will be given later.

Introduce the expression of actuator thrust in Eqs. (8), we have

$$\begin{aligned}\dot{V}_2 &= -k_1 z_{11}^2\phi_{11} - k_1 z_{21}^2\phi_{21} - k_1 z_{31}^2\phi_{31} + \frac{1}{\underline{E_1}}z_{12}\left(\phi_{12}M_{\dot{\nu}_y}\nu_y\nu_\xi/M_{\dot{\nu}_x}\right.\\ &- \phi_{12}X_{\nu_x}\nu_x/M_{\dot{\nu}_x} - \phi_{12}D_{\nu_x}\nu_x\left|\nu_x\right|/M_{\dot{\nu}_x} + \phi_{12}\tau_1/M_{\dot{\nu}_x} - \phi_{12}\dot{\alpha}_1\\ &- \left.\phi_{12}e_{12}\dot{k}/k + \phi_{12}(z_{11}\phi_{11}\cos\xi + z_{21}\phi_{21}\sin\xi)e_{12}/z_{12}\right)\\ &+ \frac{1}{\underline{E_2}}z_{22}\left(-\phi_{22}M_{\dot{\nu}_x}\nu_x\nu_\xi/M_{\dot{\nu}_y} - \phi_{22}Y_{\nu_y}\nu_y/M_{\dot{\nu}_y} + \phi_{22}\tau_2/M_{\dot{\nu}_y}\right.\\ &- \phi_{22}D_{\nu_y}\nu_y\left|\nu_y\right|/M_{\dot{\nu}_y} - \phi_{22}\dot{\alpha}_2 - \phi_{22}e_{22}\dot{k}/k + \phi_{22}(-z_{11}\phi_{11}\sin\xi\\ &+ \left.z_{21}\phi_{21}\cos\xi)e_{22}/z_{22}\right) + \frac{1}{\underline{E_3}}z_{32}\left(\phi_{32}(M_{\dot{\nu}_x} - M_{\dot{\nu}_y})\nu_x\nu_y/M_{\dot{\nu}_\xi}\right.\\ &- \phi_{32}N_{\nu_\xi}\nu_\xi/M_{\dot{\nu}_\xi} - \phi_{32}D_{\nu_\xi}\nu_\xi\left|\nu_\xi\right|/M_{\dot{\nu}_\xi} + \phi_{32}\tau_3/M_{\dot{\nu}_\xi} - \phi_{32}\dot{\alpha}_3\\ &- \left.\phi_{32}e_{32}\dot{k}/k - \phi_{32}z_{31}\phi_{31}e_{32}/z_{32}\right) - \frac{1}{\gamma}\tilde{A}\dot{\hat{A}} - \frac{1}{r}\tilde{B}\dot{\hat{B}}\\ &\le -k_1 z_{11}^2\phi_{11} - k_1 z_{21}^2\phi_{21} - k_1 z_{31}^2\phi_{31} + \frac{1}{\underline{E_1}}z_{12}\phi_{12}\tau_{1\mu}u_1/M_{\dot{\nu}_x}\\ &+ \frac{1}{\underline{E_2}}z_{22}\phi_{22}\tau_{2\mu}u_2/M_{\dot{\nu}_y} + \frac{1}{\underline{E_3}}z_{32}\phi_{32}\tau_{3\mu}u_3/M_{\dot{\nu}_\xi} + \frac{1}{\underline{E_1}}z_{12}F_1\\ &+ \frac{1}{\underline{E_2}}z_{22}F_2 + \frac{1}{\underline{E_3}}z_{32}F_3 - \frac{1}{\gamma}\tilde{A}\dot{\hat{A}} - \frac{1}{r}\tilde{B}\dot{\hat{B}}\end{aligned} \tag{29}$$

where $F_1 = \left|\phi_{12}M_{\dot{\nu}_y}\nu_y\nu_\xi/M_{\dot{\nu}_x}\right| + \left|\phi_{12}X_{\nu_x}\nu_x/M_{\dot{\nu}_x}\right| + \left|\phi_{12}D_{\nu_x}\nu_x\left|\nu_x\right|/M_{\dot{\nu}_x}\right| + \left|\phi_{12}\tau_1/M_{\dot{\nu}_x}\right| + \left|\phi_{12}\dot{\alpha}_1\right| + \left|\phi_{12}e_{12}\dot{k}/k\right| + \left|\phi_{12}(z_{11}\phi_{11}\cos\xi + z_{21}\phi_{21}\sin\xi)e_{12}/z_{12}\right|$, $F_2 = \left|\phi_{22}M_{\dot{\nu}_x}\nu_x\nu_\xi/M_{\dot{\nu}_y}\right| + \left|\phi_{22}Y_{\nu_y}\nu_y/M_{\dot{\nu}_y}\right| + \left|\phi_{22}\tau_2/M_{\dot{\nu}_y}\right| + \left|\phi_{22}D_{\nu_y}\nu_y\left|\nu_y\right|/M_{\dot{\nu}_y}\right| + \left|\phi_{22}\dot{\alpha}_2\right| + \left|-\phi_{22}e_{22}\dot{k}/k\right| + \left|\phi_{22}(-z_{11}\phi_{11}\sin\xi + z_{21}\phi_{21}\cos\xi)e_{22}/z_{22}\right|$ and $F_3 = \left|\phi_{32}(M_{\dot{\nu}_x} - M_{\dot{\nu}_y})\nu_x\nu_y/M_{\dot{\nu}_\xi}\right| + \left|\phi_{32}N_{\nu_\xi}\nu_\xi/M_{\dot{\nu}_\xi}\right| + \left|\phi_{32}D_{\nu_\xi}\nu_\xi\left|\nu_\xi\right|/M_{\dot{\nu}_\xi}\right| + \left|\phi_{32}\tau_3/M_{\dot{\nu}_\xi}\right| + \left|\phi_{32}\dot{\alpha}_3\right| + \left|\phi_{32}e_{32}\dot{k}/k\right| + \left|\phi_{32}z_{31}\phi_{31}e_{32}/z_{32}\right|$.

To avoid singularity issues, we assume $z_{12}(0)$, $z_{22}(0)$ and $z_{32}(0)$ are not equal to zeros. According to Lemma 1, for any given $\varepsilon_i > 0$, the following equation exists

$$F_1 = W_1^T\Lambda_1(\sigma_1) + \delta_1(\sigma_1), \delta_1(\sigma_1) \le \varepsilon_1 \tag{30}$$

$$F_2 = W_2^T\Lambda_2(\sigma_2) + \delta_2(\sigma_2), \delta_2(\sigma_2) \le \varepsilon_2 \tag{31}$$

$$F_3 = W_3^T\Lambda_3(\sigma_3) + \delta_3(\sigma_3), \delta_3(\sigma_3) \le \varepsilon_3 \tag{32}$$

where, $\delta_i(\sigma_i)$ denotes the approximation error, $\sigma_1 = \left[x, y, \xi, \nu_x, \nu_y, \nu_\xi, x_d, y_d, \dot{x}_d, \dot{y}_d\right]^T$, $\sigma_2 = \left[x, y, \xi, \nu_x, \nu_y, \nu_\xi, x_d, y_d, \dot{x}_d, \dot{y}_d\right]^T$, $\sigma_3 = \left[\xi, \nu_x, \nu_y, \nu_\xi, \xi_d, \dot{\xi}_d\right]^T$. Then, we have

$$\begin{aligned}\dot{V}_2 &\le -k_1 z_{11}^2\phi_{11} - k_1 z_{21}^2\phi_{21} - k_1 z_{31}^2\phi_{31} + \frac{1}{\underline{E_1}}z_{12}E_1u_1 + \frac{1}{\underline{E_2}}z_{22}E_2u_2\\ &+ \frac{1}{\underline{E_3}}z_{32}E_3u_3 + \frac{1}{\underline{E_1}}z_{12}W_1^T\Lambda_1(\sigma_1) + \frac{1}{\underline{E_2}}z_{22}W_2^T\Lambda_2(\sigma_2)\\ &+ \frac{1}{\underline{E_3}}z_{32}W_3^T\Lambda_3(\sigma_3)\\ &+ \frac{1}{\underline{E_1}}z_{12}\delta_1(\sigma_1) + \frac{1}{\underline{E_2}}z_{22}\delta_2(\sigma_2) + \frac{1}{\underline{E_3}}z_{32}\delta_3(\sigma_3) - \frac{1}{\gamma}\tilde{A}\dot{\hat{A}} - \frac{1}{r}\tilde{B}\dot{\hat{B}}\end{aligned} \tag{33}$$

where $E_1 = \phi_{12}\tau_{1\mu}/M_{\dot{\nu}_x}$, $E_2 = \phi_{22}\tau_{2\mu}/M_{\dot{\nu}_y}$, $E_3 = \phi_{32}\tau_{3\mu}/M_{\dot{\nu}_\xi}$.

In traditional adaptive neural control methods, three independent adaptive neural network modules should be used for the AUV system to improve the control performance, which may lead to a high calculation load. Thus, the simplification problem of the adaptive neural controllers is considered in this paper. According to Lemma 2, it is apparent that

$$\begin{aligned}\frac{1}{\underline{E_i}}z_{i2}W_i^T\Lambda_i(\sigma_i) &\le \frac{1}{\underline{E_i}}\left|z_{i2}\right|\left\|W_i\right\|\left\|\Lambda_i(\sigma_i)\right\|\\ &\le \frac{1}{\underline{E_i}}\left|z_{i2}\right|\left\|W_i\right\|\left\|\Lambda_i(\bar{\sigma})\right\|\\ &\le A\left|z_{i2}\right|\left\|\Lambda(\bar{\sigma})\right\|\end{aligned} \tag{34}$$

where $\bar{\sigma} = \left[\xi, \nu_x, \nu_y, \nu_\xi\right]^T$ and $A = \max\left\{\frac{\|W_1\|}{\underline{E_1}}, \frac{\|W_2\|}{\underline{E_2}}, \frac{\|W_3\|}{\underline{E_3}}\right\}$. In this paper, for the same input signal, we choose the same center of the

receptive field and number of nodes for the neural network. To simplify the expression, we use Λ for $\Lambda(\bar{\sigma})$. According to Lemma 3, one has

$$\begin{aligned}|z_{i2}|\,\|\Lambda\| &\le \frac{z_{i2}^2\Lambda^T\Lambda}{\sqrt{z_{i2}^2\Lambda^T\Lambda+o^2}}+o\\ &= G_i+o\end{aligned} \tag{35}$$

where $G_i = \frac{z_{i2}^2\Lambda^T\Lambda}{\sqrt{z_{i2}^2\Lambda^T\Lambda+o^2}}$. Then, according to Eqs. (34)–(35) and Lemma 3, we have

$$\begin{aligned}\dot{V}_2 &\le -k_1z_{11}^2\phi_{11}-k_1z_{21}^2\phi_{21}-k_1z_{31}^2\phi_{31}+\frac{1}{\underline{E_1}}z_{12}E_1u_1+\frac{1}{\underline{E_2}}z_{22}E_2u_2\\ &+\frac{1}{\underline{E_3}}z_{32}E_3u_3+A\left(G_1+G_2+G_3\right)+3Ao+B\left(|z_{21}|+|z_{22}|+|z_{32}|\right)\\ &-\frac{1}{\gamma}\tilde{A}\dot{\hat{A}}-\frac{1}{r}\tilde{B}\dot{\hat{B}}\\ &\le -k_1z_{11}^2\phi_{11}-k_1z_{21}^2\phi_{21}-k_1z_{31}^2\phi_{31}+\frac{E_1}{\underline{E_1}}z_{12}\left(-k_2z_{12}-\frac{z_{12}\Lambda^T\Lambda\hat{A}}{\sqrt{z_{12}^2\Lambda^T\Lambda+o^2}}\right.\\ &\left.-\frac{z_{12}\hat{B}^2}{\sqrt{z_{12}^2\hat{B}^2+o^2}}\right)+\frac{E_2}{\underline{E_2}}z_{22}\left(-k_2z_{22}-\frac{z_{22}\Lambda^T\Lambda\hat{A}}{\sqrt{z_{22}^2\Lambda^T\Lambda+o^2}}-\frac{z_{22}\hat{B}^2}{\sqrt{z_{22}^2\hat{B}^2+o^2}}\right)\\ &+\frac{E_3}{\underline{E_3}}z_{32}\left(-k_2z_{32}-\frac{z_{32}\Lambda^T\Lambda\hat{A}}{\sqrt{z_{32}^2\Lambda^T\Lambda+o^2}}\;-\frac{z_{32}\hat{B}^2}{\sqrt{z_{32}^2\hat{B}^2+o^2}}\right)+A\left(G_1+G_2\right.\\ &\left.+G_3\right)+3Ao+B\left(|z_{12}|+|z_{22}|+|z_{32}|\right)-\frac{1}{\gamma}\tilde{A}\dot{\hat{A}}-\frac{1}{r}\tilde{B}\dot{\hat{B}}\\ &\le -k_1z_{11}^2\phi_{11}-k_1z_{21}^2\phi_{21}-k_1z_{31}^2\phi_{31}-k_2z_{12}^2-k_2z_{22}^2-k_2z_{32}^2-\hat{A}\left(G_1\right.\\ &\left.+G_2+G_3\right)-\frac{z_{12}^2\hat{B}^2}{\sqrt{z_{12}^2\hat{B}^2+o^2}}-\frac{z_{22}^2\hat{B}^2}{\sqrt{z_{22}^2\hat{B}^2+o^2}}-\frac{z_{32}^2\hat{B}^2}{\sqrt{z_{32}^2\hat{B}^2+o^2}}\\ &+A\left(G_1+G_2+G_3\right)+3Ao+B\left(|z_{12}|+|z_{22}|+|z_{32}|\right)-\frac{1}{\gamma}\tilde{A}\dot{\hat{A}}-\frac{1}{r}\tilde{B}\dot{\hat{B}}\\ &\le -k_1z_{11}^2\phi_{11}-k_1z_{21}^2\phi_{21}-k_1z_{31}^2\phi_{31}-k_2z_{12}^2-k_2z_{22}^2-k_2z_{32}^2\\ &+(3+3A)\,o\\ &+\frac{1}{\gamma}\tilde{A}\left(\gamma\left(G_1\;+G_2+G_3\right)-\dot{\hat{A}}\right)+\frac{1}{r}\tilde{B}\left(r\left(|z_{12}|+|z_{22}|+|z_{32}|\right)-\dot{\hat{B}}\right)\\ &\le -k_1z_{11}^2\phi_{11}-k_1z_{21}^2\phi_{21}-k_1z_{31}^2\phi_{31}-k_2z_{21}^2-k_2z_{22}^2-k_2z_{32}^2\\ &+\left(3+3A+\tilde{A}\hat{A}+\tilde{B}\hat{B}\right)o\end{aligned} \tag{36}$$

where $B=\max\left\{\frac{\varepsilon_1}{\underline{E_1}},\frac{\varepsilon_2}{\underline{E_2}},\frac{\varepsilon_3}{\underline{E_3}}\right\}$ (see Fig. 1).

Thus, our control laws and the corresponding adaptive laws are

$$u_1=-k_2z_{12}-\frac{z_{12}\Lambda^T\Lambda\hat{A}}{\sqrt{z_{12}^2\Lambda^T\Lambda+o^2}}-\frac{z_{12}\hat{B}^2}{\sqrt{z_{12}^2\hat{B}^2+o^2}} \tag{37}$$

$$u_2=-k_2z_{22}-\frac{z_{22}\Lambda^T\Lambda\hat{A}}{\sqrt{z_{22}^2\Lambda^T\Lambda+o^2}}-\frac{z_{22}\hat{B}^2}{\sqrt{z_{22}^2\hat{B}^2+o^2}} \tag{38}$$

$$u_3=-k_2z_{32}-\frac{z_{32}\Lambda^T\Lambda\hat{A}}{\sqrt{z_{32}^2\Lambda^T\Lambda+o^2}}-\frac{z_{32}\hat{B}^2}{\sqrt{z_{32}^2\hat{B}^2+o^2}} \tag{39}$$

$$\dot{\hat{A}}=\gamma\left(G_1+G_2+G_3\right)-\gamma o\hat{A} \tag{40}$$

$$\dot{\hat{B}}=r\left(|z_{12}|+|z_{22}|+|z_{32}|\right)-ro\hat{B} \tag{41}$$

where $o(t)$ is a nonlinear function that satisfies $\lim_{t\to\infty}\int_0^t o(t)ds\le\bar{o}\le\infty$ with a constant $\bar{o}>0$. In this paper, $o(t)$ is set to $o(t)=\frac{1}{t^2+0.1}$ is selected. Thus, the structure of our control system can be shown in Fig. 2.

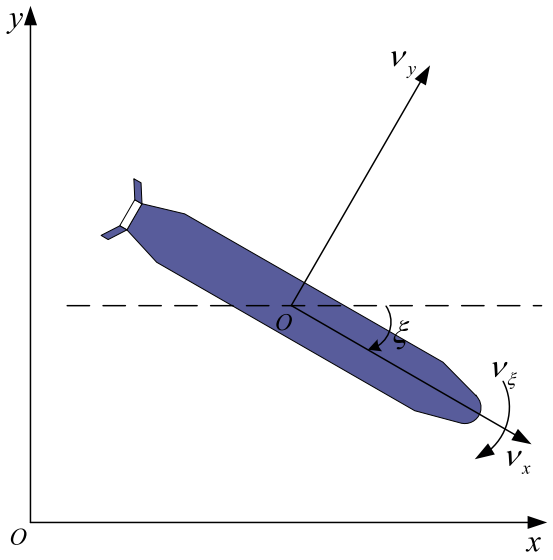

Fig. 1. Body-fixed of AUVs and earth-fixed coordinate systems.

4. System performance analysis

In this section, the system asymptotic stability is analyzed. In the first step, we illustrate that the AUV system (1)–(6) under our control method (37)–(39) and the updating law (40)–(41) has a unique solution for a time interval $[0,t_{\max})$. And then, the second step is given to show that $t_{\max}=+\infty$. Finally, it is proved that the asymptotic tracking control is realized in this paper.

Define the compact form as

$$\Omega=\left[z_{11},z_{21},z_{31},z_{12},z_{22},z_{32},\hat{A},\hat{B}\right]^T \tag{42}$$

Thus, the vector $\dot{\Omega}$ can be easily obtained from (22)–(24) and (37)–(39).

$$\dot{\Omega}=h(t,\Omega)=\begin{bmatrix}h_1\left(t,z_{11}\right)\\ h_2\left(t,z_{21}\right)\\ h_3\left(t,z_{31}\right)\\ h_4\left(t,z_{11},z_{21},z_{12},\hat{A},\hat{B}\right)\\ h_5\left(t,z_{11},z_{21},z_{22},\hat{A},\hat{B}\right)\\ h_6\left(t,z_{31},z_{32},\hat{A},\hat{B}\right)\\ h_7\left(t,z_{12},z_{22},z_{32},\hat{A}\right)\\ h_8\left(t,z_{12},z_{22},z_{32},\hat{B}\right)\end{bmatrix}. \tag{43}$$

Define an open set

$$N=\underbrace{\left(-\theta_s,\theta_u\right)\times\cdots\times\left(-\theta_s,\theta_u\right)}_{6}\times R\times R \tag{44}$$

It is obvious that $\Omega(0)=\left[0,0,0,0,0,0,\hat{A}^0,\hat{B}^0\right]^T\in N$. It is noted that the desired trajectories x_d, y_d, ξ_d, the pre-defined function k and the nonlinear function $\Phi\left(Q_{ij}\right)$ are bounded, continuous and differentiable. Thus, $M_{\dot{v}_x}$, $M_{\dot{v}_y}$, $M_{\dot{v}_\xi}$, I_z, $X_{\dot{v}_x}$, $Y_{\dot{v}_y}$, $N_{\dot{v}_\xi}$, X_{v_x}, Y_{v_y}, N_{v_ξ}, D_{v_x}, D_{v_y}, D_{v_ξ} are continuous in t and locally Lipschitz in x, y, ξ, v_x, v_y and v_ξ. Hence, the local Lipschitz condition for the nonlinear function $h(t,\Omega)$ is satisfied. Based on Theorem 54 in Sontag (1998), the unique solution Ω can be guaranteed during a time interval $[0,t_{\max})$.

According to perfect square formula, the following inequalities hold

$$\tilde{A}\hat{A}=\tilde{A}\left(A-\tilde{A}\right)=-\tilde{A}^2+\tilde{A}A\le\frac{A^2}{4} \tag{45}$$

$$\tilde{B}\hat{B}=\tilde{B}\left(B-\tilde{B}\right)=-\tilde{B}^2+\tilde{B}B\le\frac{B^2}{4} \tag{46}$$

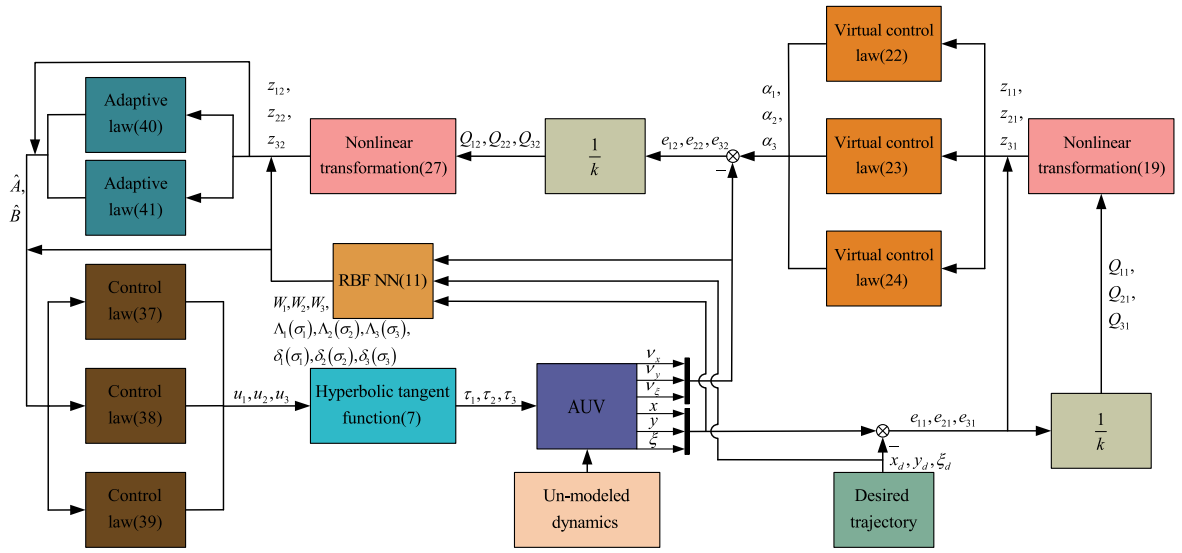

Fig. 2. Structure of our control method.

From Eqs. (45)–(46), one has

$$\dot{V}_2 \le -k_1 z_{11}^2 \phi_{11} - k_1 z_{21}^2 \phi_{21} - k_1 z_{31}^2 \phi_{31} - k_2 z_{12}^2 - k_2 z_{22}^2 - k_2 z_{32}^2 + \left(3 + 3A + \left(A^2 + B^2\right)/4\right) o \tag{47}$$

By integrating Eqs. (47), we have

$$\begin{aligned} &V_2(t) + \int_0^t k_1 z_{11}^2(s)\phi_{11}(s)ds + \int_0^t k_1 z_{21}^2(s)\phi_{21}(s)ds \\ &+ \int_0^t k_1 z_{31}^2(s)\phi_{31}(s)ds + \int_0^t k_2 z_{12}^2(s)ds + \int_0^t k_2 z_{22}^2(s)ds \\ &+ \int_0^t k_2 z_{32}^2(s)ds \\ &\le V_2(0) + \left(3 + 3A + \left(A^2 + B^2\right)/4\right) \int_0^t o(s)ds \end{aligned} \tag{48}$$

Then, it is derived as

$$\frac{1}{2} z_{11}^2 \le V_2 \le V_2(0) + \left(3 + 3A + \left(A^2 + B^2\right)/4\right) \bar{o} \tag{49}$$

Let $\varpi = V_2(0) + \left(3 + 3A + \left(A^2 + B^2\right)/4\right) \bar{o}$. And then, we have

$$\frac{1}{2} z_{21}^2 \le V_2 \le \varpi \tag{50}$$

$$\frac{1}{2} z_{31}^2 \le V_2 \le \varpi \tag{51}$$

$$\frac{1}{2E_1} z_{12}^2 \le V_2 \le \varpi \tag{52}$$

$$\frac{1}{2E_2} z_{22}^2 \le V_2 \le \varpi \tag{53}$$

$$\frac{1}{2E_3} z_{32}^2 \le V_2 \le \varpi \tag{54}$$

$$\frac{1}{2\gamma} \tilde{A}^2 \le V_2 \le \varpi \tag{55}$$

$$\frac{1}{2r} \tilde{B}^2 \le V_2 \le \varpi \tag{56}$$

From Eqs. (49)–(56), for $\forall t \in [0, t_{\max})$, results into

$$|z_{11}| \le \bar{z}_{11} = \sqrt{2\varpi} \tag{57}$$

$$|z_{21}| \le \bar{z}_{21} = \sqrt{2\varpi} \tag{58}$$

$$|z_{31}| \le \bar{z}_{31} = \sqrt{2\varpi} \tag{59}$$

$$|z_{12}| \le \bar{z}_{12} = \sqrt{2E_1\varpi} \tag{60}$$

$$|z_{22}| \le \bar{z}_{22} = \sqrt{2E_2\varpi} \tag{61}$$

$$|z_{32}| \le \bar{z}_{32} = \sqrt{2E_3\varpi} \tag{62}$$

$$\left|\hat{A}\right| \le \bar{\hat{A}} = \sqrt{2\gamma\varpi} + A \tag{63}$$

$$\left|\hat{B}\right| \le \bar{\hat{B}} = \sqrt{2r\varpi} + B \tag{64}$$

Therefore, for $\forall t \in [0, t_{\max})$, it can be inferred that z_{ij}, α_i and u_i are bounded. Consider a set $N' = \left[-\bar{z}_{11}, \bar{z}_{11}\right] \times \left[-\bar{z}_{21}, \bar{z}_{21}\right] \times \left[-\bar{z}_{31}, \bar{z}_{31}\right] \times \left[-\bar{z}_{12}, \bar{z}_{12}\right] \times \left[-\bar{z}_{22}, \bar{z}_{22}\right] \times \left[-\bar{z}_{32}, \bar{z}_{32}\right] \times \left[-\bar{\hat{A}}, \bar{\hat{A}}\right] \times \left[-\bar{\hat{B}}, \bar{\hat{B}}\right] \subset N$. Thus, during the time interval $[0, t_{\max})$, the AUV system has a only maximum solution $\Omega \in N'$. In addition, k, $\dot{k}$, x_d, y_d, ξ_d, $\dot{x}_d$, $\dot{y}_d$, $\dot{\xi}_d$, x, y, ξ, v_x, v_y, v_ξ and $\dot{\alpha}_i$ are bounded. By virtue of Proposition C.3.6 given in Sontag (1998), $t_{\max} = +\infty$ is obtained. From the definition of e_{i1}, the boundedness of $\dot{e}_{i1}$ can be easily guaranteed. Thus, $\lim_{t\to\infty} e_{i1} = 0$ is proven based on Barbalat lemma (Min and Liu, 2007). Namely, the proposed controller makes AUV realize the asymptotic adaptive tracking control.

Remark 1. A novel single neural network-based adaptive control strategy is proposed for AUVs in this paper. All the parameters in the AUV system are not required in our controller. Compared with existing results that using multi-neural approximators (Yu et al., 2020; Liu et al., 2022; Yan et al., 2019; Kim and Yoo, 2021), our control method has a relatively smaller computational burden.

Remark 2. A new compensation mechanism (23) is incorporating into the neural control method to overcome the approximation error of neural network. And the nonlinear transformation (16) is also employed in the backstepping-based framework to enhance the control ability. Thus, both the asymptotic tracking control stability and the transient response performance can be guaranteed under our control strategy.

Remark 3. The inertia tensor coefficients are completely unknown in this paper. Thus, the results that focus on the strictly-feedback nonlinear systems with the known control gains cannot be extended to the AUV systems directly (Lai et al., 2016; Liu et al., 2022). Furthermore, compared with the works that only guarantee the ultimate boundedness of the tracking errors, the asymptotic convergence of the tracking errors is ensured by employing the neural control functions (37)–(39) and the updating laws (40)–(41).

5. Simulation results

Simulation results are displayed to evaluate the trajectory tracking performance of AUVs under our control strategy. The system parameters for the AUV given in Shen et al. (2018) are $D_{v_y} = 503.8$ kg/m,

$D_{v_x} = 241.3$ kg/m, $D_{v_\xi} = 76.9$ kg m^2/rad^2, $I_z = 13.1$ kg m^2, $N_{\dot{v}_\xi} = -15.9$ kg m^2, $N_{v_\xi} = 3.5$ kg m^2/(s rad), $Y_{\dot{v}_y} = -477.2$ kg, $Y_{v_y} = 35.8$ kg/s, $X_{\dot{v}_x} = -167.6$ kg, $X_{v_x} = 26.9$ kg/s, $u_M = 30$ N, and $m = 116$ kg. The reference trajectories are defined as $x_d = \sin(0.1t)$, $y_d = \cos(0.05t)$, $\xi_d = \text{atan}\,2(-0.05sin(0.05t), 0.1cos(0.1t))$.

During the simulation, the initial values for the AUV system are $x(0) = y(0) = \xi(0) = 0$, $v_x(0) = v_y(0) = v_\xi(0) = 0$, $x_d(0) = 0$, $y_d(0) = 1$ and $\xi_d(0) = 0$. Our control parameters are determined based on the trial-and-error method. Firstly, all the parameters in our controller are set to zeros to obtain the simulation results. And then, the pre-defined region is given by choosing the parameters in (19) and (18). Next, we will determine the values of parameters in the neural network and adaptive laws. As the author knows, there is no universal way to design a neural network for the AUV systems. Thus, the number of NN nodes and the Gaussian function widths should be repeatedly adjusted based on the simulation results. In the final, the control gains k_1 and k_2 are determined to further improve the system performance. More information about the influence of control parameters can refer to the result in Zheng and Yang (2020). Hence, our controller parameters can be given by $\iota = 0.1$, $k_0 = 10$, $k_\infty = 0.1$, $\theta_u = 1$, $\theta_s = 1$, $k_1 = 5$, $k_2 = 100$, $r = 0.001$ and $\gamma = 0.001$. And the function $o(t)$ is $o(t) = \frac{1}{t^2+0.1}$. The neural network parameters are $N = 7$, $n = 4$, $x_1 = \xi$, $x_2 = v_x$, $x_3 = v_y$, $x_4 = v_\xi$, $h_{1p} = 1.5$, $h_{2p} = 1$, $h_{3p} = 0.5$, $h_{4p} = 0$, $h_{5p} = -0.5$, $h_{6p} = -1$, $h_{7p} = -1.5$ and $\mu = 2$.

With the above control parameters, we carried out two groups of simulation experiments on the MATLAB platform. In the first case, the response curves of all the signals in the AUV are displayed to show the effectiveness of our strategy. Furthermore, the comparisons between our controller, the dynamic surface control strategy (DSC) (von Ellenrieder, 2019) and the neural adaptive control method (NN) (Chen et al., 2009) are given to show the advantage of the proposed scheme. And then, in order to further illustrate the ability of our controller to eliminate the uncertain dynamics, there exists 30% system parameter errors in Simulation 2.

Simulation 1. The results of the simulation are illustrated in Figs. 3–10. The tracking signals of x direction, y direction and ξ are shown in Figs. 3–5 respectively. Fig. 6 depicts the curve of the AUV in the xoy coordinate system. Fig. 7 describes the response curve of speed signals, and Fig. 8 shows the tracking error of AUVs. From the simulation results, we can find that the maximum tracking errors between x and x_d, y and y_d, ξ and ξ_d are 0.2857, 1 and 0.0551 respectively. And, the average absolute values for e_{11}, e_{21} and e_{31} are 0.0092, 0.0245 and 0.0018 respectively. Thus, we can conclude that the tracking errors are restricted to a preset region. Our control command signals generated by the controller are shown in Fig. 9, and the adaptive law signals are shown in Fig. 10. The comparison results between our controller and existing methods (Chen et al., 2009; von Ellenrieder, 2019) are also given in Figs. 3–6. Obviously, compared with the traditional neural network (Chen et al., 2009) and dynamic surface control strategy (von Ellenrieder, 2019), our scheme has a better control performance. In order to illustrate the advantage of our method in saving computing resources, the calculation times of different control methods are given in Table 1. We run the simulation codes in the same Matlab platform 100 times, and the average running time is used to show the computational complexity of the control method. Compared with the NN controller, the calculation time of our control strategy is only 1.8 s. The main reason for this phenomenon is that our controller only needs one neural network and two adaptive laws, while the NN control strategy should calculate three neural networks and three updating laws.

Remark 4. Compared with existing adaptive neural approaches (Zhao et al., 2018; Liu et al., 2022; Zheng and Yang, 2020; Xu et al., 2022), our control strategy is able to reduce the number of neural networks. In virtue of dynamic compensation law (41), the zero-error regulation

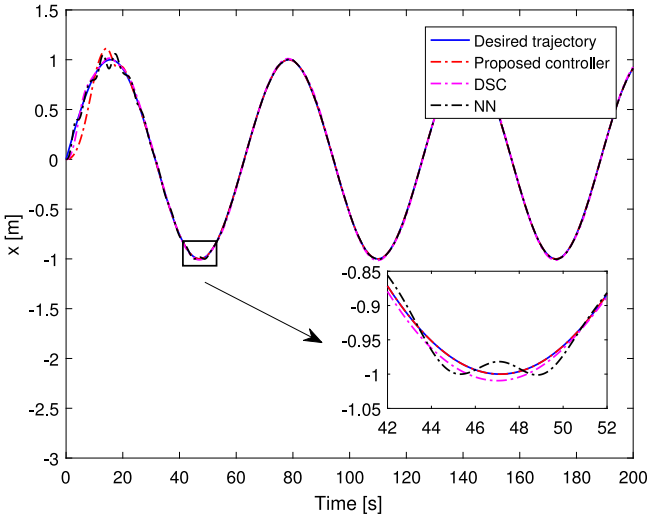

Fig. 3. Response curves of x-direction actual signals in Simulation 1.

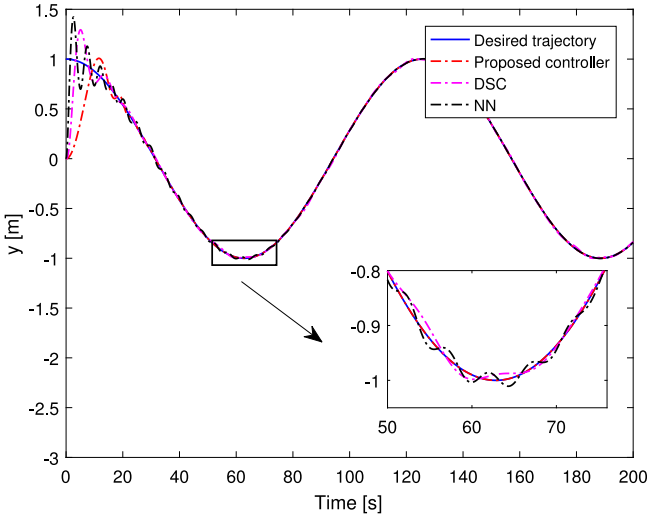

Fig. 4. Response curves of y-direction actual signals in Simulation 1.

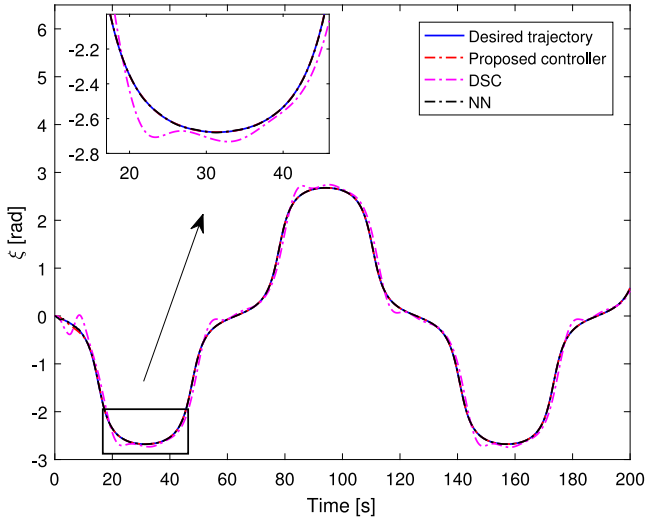

Fig. 5. Response curves of signals ξ in Simulation 1.

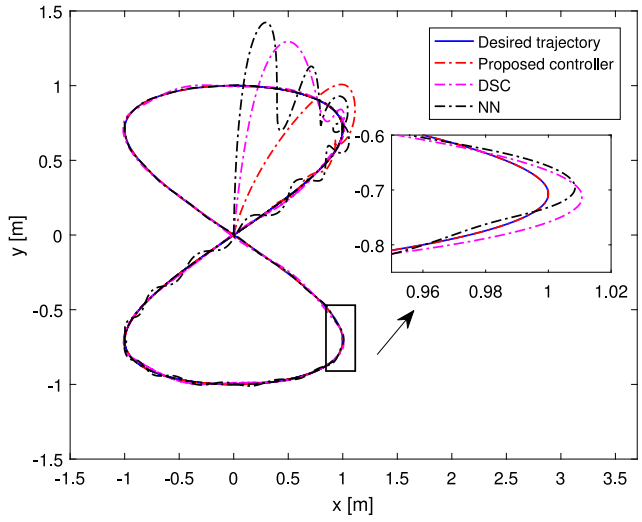

Fig. 6. Tracking responses of AUVs in the xoy plane in Simulation 1.

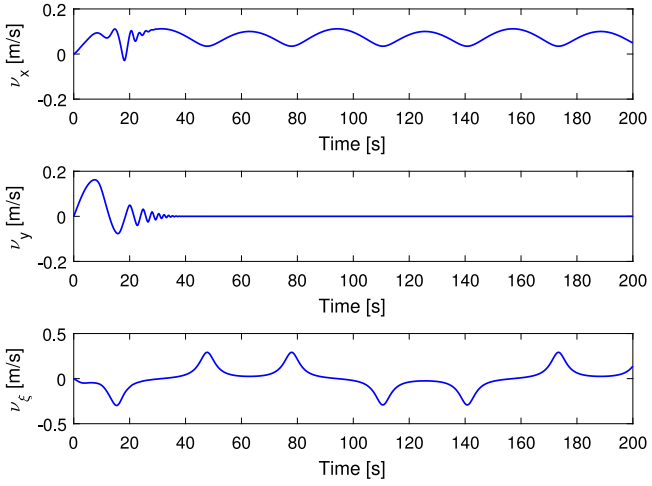

Fig. 7. Response curves of speed signals in Simulation 1.

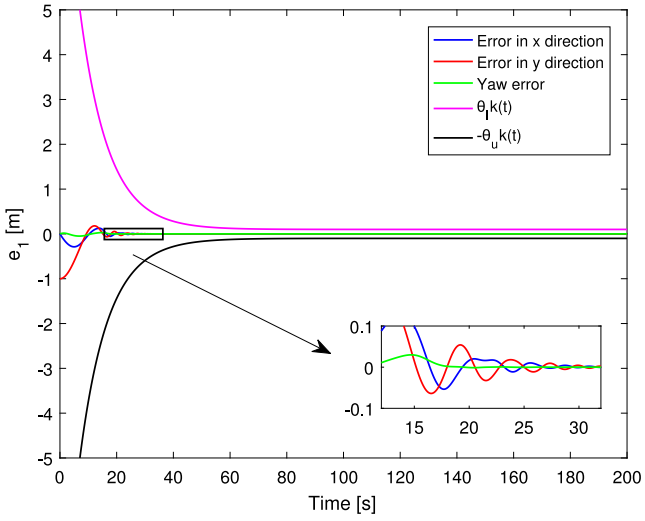

Fig. 8. Response curves of control errors of AUVs in Simulation 1.

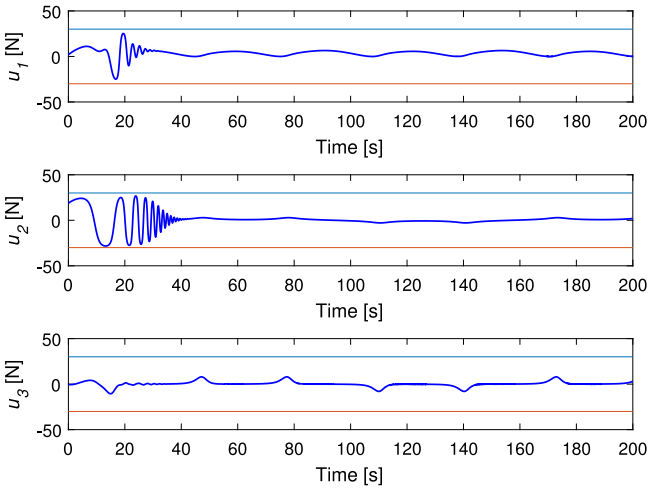

Fig. 9. Curves of the control signals in Simulation 1.

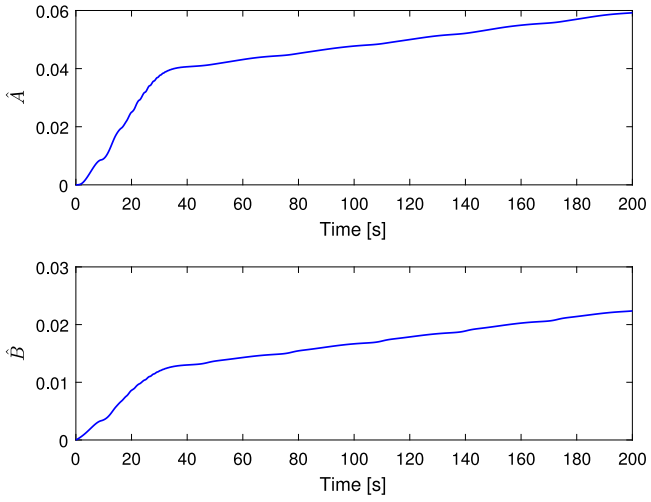

Fig. 10. Response curves of adaptive law signals in Simulation 1.

Table 1
Comparison results for different control strategies.

	Our controller	DSC	NN
Average calculation time	1.8 s	0.7 s	2.8 s
Number of NNs	1	0	3
Number of adaptive laws	2	0	3

Table 2
Control performance under different neural networks node numbers.

The number of neural nodes	7	13	16	25
Mean absolute error (e_{11})	0.0092	0.0051	0.0043	0.0028
Mean absolute error (e_{21})	0.0245	0.0135	0.0114	0.0074
Mean absolute error (e_{31})	0.0018	0.0009	0.0008	0.0005

of the adaptive NN method can also be ensured. From the simulation results given in Figs. 3–6, the AUV system can track the given references more quickly under our control method. Thus, our strategy has a better performance.

Remark 5. As shown in Table 2, the tracking errors under our method decreased with the number of NN nodes rising. However, the complexity of our control strategy is also increased with the node numbers

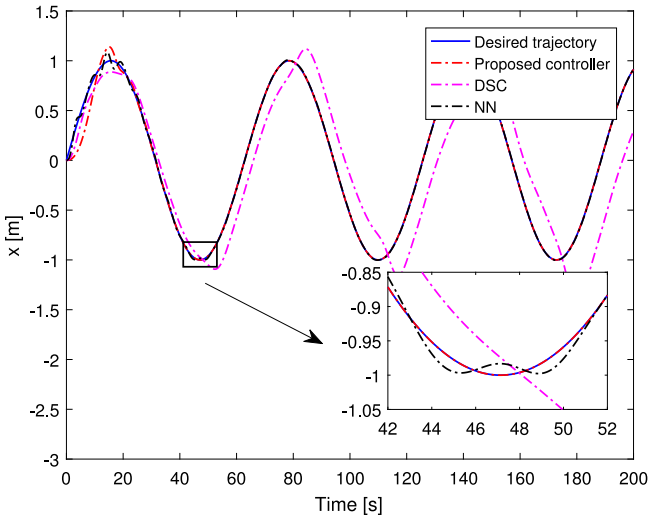

Fig. 11. Response curves of x-direction actual signals in Simulation 2.

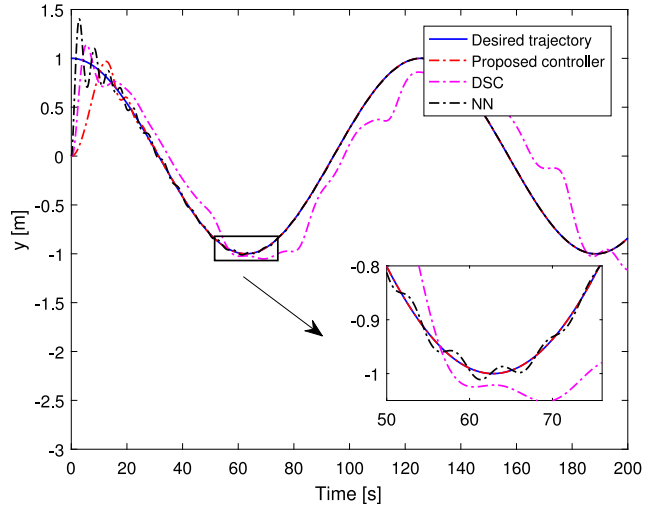

Fig. 12. Response curves of y-direction actual signals in Simulation 2.

as well. Thus, the design of neural networks should consider both the control complexity and the system performance.

Simulation 2. To further verify the effectiveness of our method, there are 30% model parameter errors for the tested AUV system in this case. The simulation results are shown in Figs. 11–18. The actual tracking behaviors of AUVs are given in Figs. 11–14. The average values for $|e_{11}|$, $|e_{21}|$ and $|e_{31}|$ are 0.0108, 0.0271 and 0.0021 respectively. Thus, our controller is able to eliminate the influence of system uncertainty on the AUV's performance. The speed signals, control command signals, tracking error and adaptive signals of AUVs are shown in Figs. 15–18 respectively. The maximum absolute errors for e_{11}, e_{21} and e_{31} are 0.3116, 1 and 0.0573 respectively. It can be seen that even though there are 30% parameter errors in the system model, the AUV can still track the desired trajectory accurately. Furthermore, the comparison results shown in Figs. 11–14 also illustrate that our controller has a stronger robustness than the existing control strategies (Chen et al., 2009; von Ellenrieder, 2019).

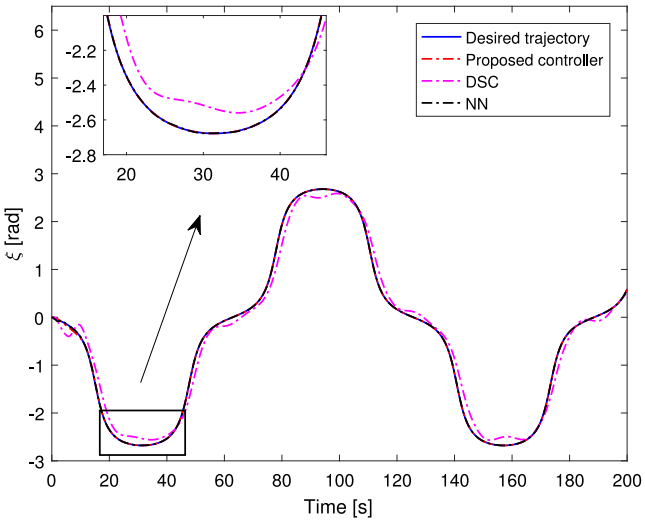

Fig. 13. Response curves of signals ξ in Simulation 2.

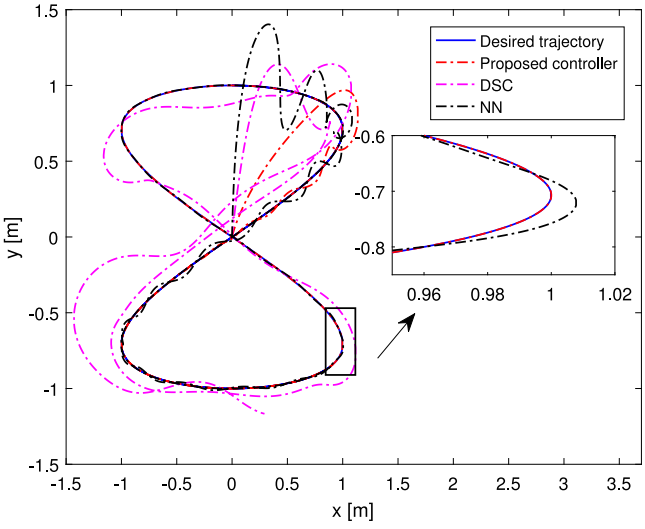

Fig. 14. Tracking responses of AUVs in the xoy plane in Simulation 2.

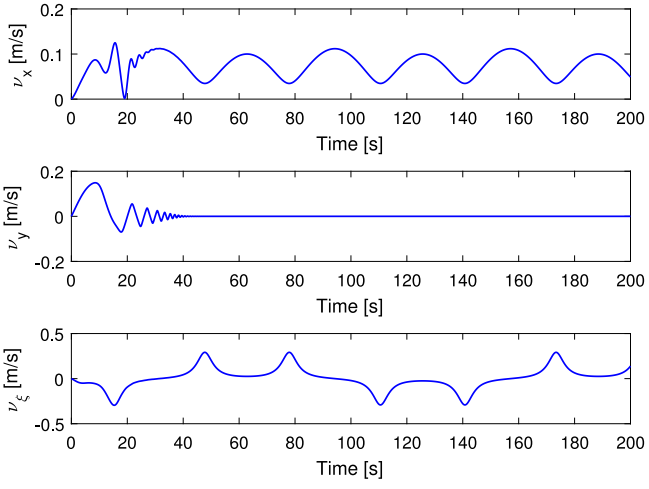

Fig. 15. Response curves of speed signals in Simulation 2.

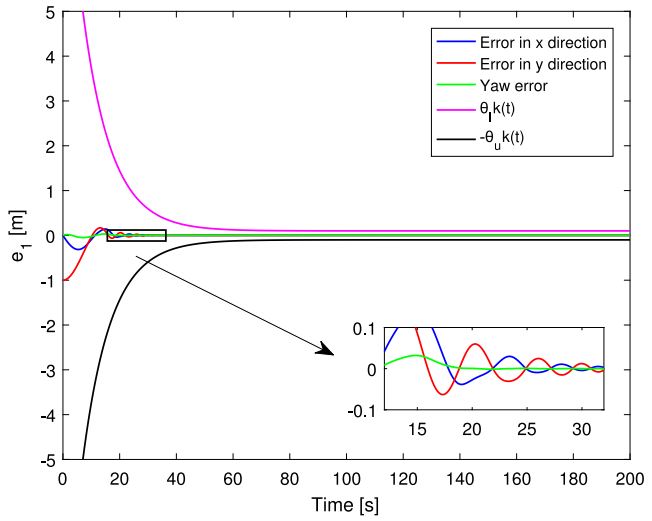

Fig. 16. Response curves of control error of AUVs in Simulation 2.

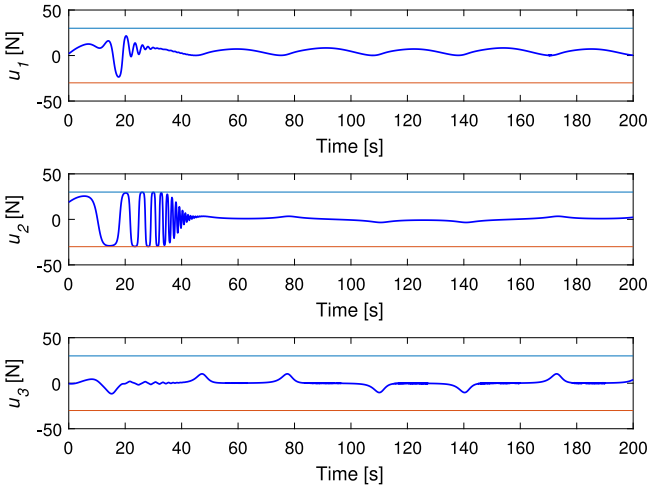

Fig. 17. Curves of the control signals in Simulation 2.

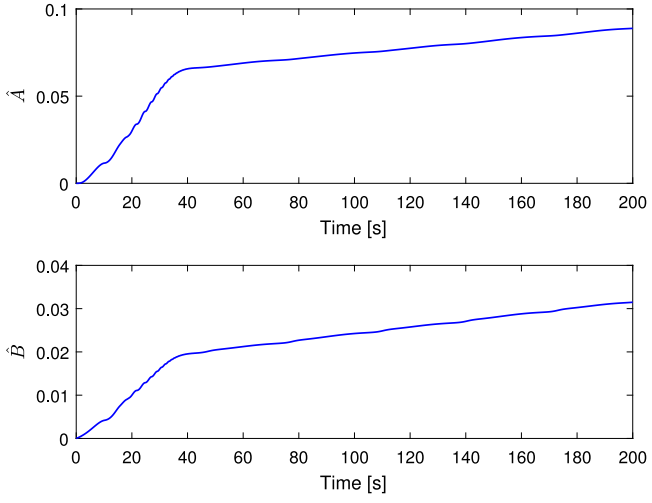

Fig. 18. Response curves of adaptive law signals in Simulation 2.

6. Conclusions

A novel asymptotic adaptive neural network control algorithm is proposed for the AUV with un-modeled dynamics and input saturation. Compared with existing results, only one neural network and two adaptive laws are employed to overcome the un-modeled dynamic problem, which decreases the computation burden of the control system. Besides, the control performance is improved by adopting the nonlinear transformation method in the backstepping-based control framework. Thus, the asymptotic convergence of tracking errors is proven based on the Lyapunov analysis. Finally, the effectiveness of our control method is illustrated by analyzing the simulation results.

CRediT authorship contribution statement

Yuxi Zhang: Conceptualization, Methodology, Writing – original draft. **Jiapeng Liu:** Conceptualization, Methodology, Funding acquisition, Project administration, Writing – review & editing. **Jinpeng Yu:** Methodology, Funding acquisition, Writing – review & editing. **Dongxiao Liu:** Writing – review & editing.

Declaration of competing interest

The authors declare that they have no known competing financial interests or personal relationships that could have appeared to influence the work reported in this paper.

Data availability

No data was used for the research described in the article.

Acknowledgments

This work is supported in part by the Natural Science Foundation of Shandong Province (No. ZR2020QF063), in part by the National Natural Science Foundation of China (61973179), in part by the Chang Jiang scholars Program, in part by the Taishan Scholar Special Project fund under Grant TSTP20221120, in part by the Major Innovation Project of Shandong Province under Grant 2022CXGC020901, in part by the Qingdao Key Technology Research and Industrialization Demonstration Project under Grant 23-1-4-xxgg-6-gx and in part by the Taishan Scholar Special Project Fund.

References

Che, G., Yu, Z., 2020. Neural-network estimators based fault-tolerant tracking control for AUV via ADP with rudders faults and ocean current disturbance. Neurocomputing 411, 442–454.

Chen, B., Liu, X., Liu, K., Lin, C., 2009. Novel adaptive neural control design for nonlinear MIMO time-delay systems. Automatica 45, 1554–1560.

Choi, Y.H., Yoo, S.J., 2019. An improved design strategy for approximation-based adaptive event-triggered tracking of a class of uncertain nonlinear systems. J. Franklin Inst. B 356, 4378–4396.

Ding, Z., Wang, H., Sun, Y., Qin, H., 2022. Adaptive prescribed performance second-order sliding mode tracking control of autonomous underwater vehicle using neural network-based disturbance observer. Ocean Eng. 260, 111939.

Elhaki, O., Shojaei, K., 2018. Neural network-based target tracking control of underactuated autonomous underwater vehicles with a prescribed performance. Ocean Eng. 167, 239–256.

von Ellenrieder, K.D., 2019. Dynamic surface control of trajectory tracking marine vehicles with actuator magnitude and rate limits. Automatica 105, 433–442.

Fang, Y., Huang, Z., Pu, J., Zhang, J., 2022. AUV position tracking and trajectory control based on fast-deployed deep reinforcement learning method. Ocean Eng. 245, 110452.

Fischer, N., Hughes, D., Walters, P., Schwartz, E.M., Dixon, W.E., 2014. Nonlinear RISE-based control of an autonomous underwater vehicle. IEEE Trans. Robot. 30, 845–852.

Fossen, T.I., 2002. Marine Control Systems: Guidance, Navigation and Control of Ships, Rigs and Underwater Vehicles. Marine Cybernetics, Trondheim, Norway.

Kim, J.H., Yoo, S.J., 2021. Distributed event-driven adaptive three-dimensional formation tracking of networked autonomous underwater vehicles with unknown nonlinearities. Ocean Eng. 233, 109069.

Lai, G., Liu, Z., Chen, C.P., Zhang, Y., 2016. Adaptive asymptotic tracking control of uncertain nonlinear system with input quantization. Systems Control Lett. 96, 23–29. http://dx.doi.org/10.1016/j.sysconle.2016.06.010.

Li, J., Du, J., Chang, W.J., 2019. Robust time-varying formation control for underactuated autonomous underwater vehicles with disturbances under input saturation. Ocean Eng. 179, 180–188. http://dx.doi.org/10.1016/j.oceaneng.2019.03.017.

Liu, J., Wang, Q.G., Yu, J., 2022. Event-triggered adaptive neural network tracking control for uncertain systems with unknown input saturation based on command filters. IEEE Trans. Neural Netw. Learn. Syst. 1, 1–6. http://dx.doi.org/10.1109/TNNLS.2022.3224065.

Min, Y.Y., Liu, Y.G., 2007. Barbalat lemma and its application in analysis of system stability. J. Shandong Univ. (Eng. Sci.) 37, 51–55.

Mohammadi, M., Arefi, M.M., Vafamand, N., Kaynak, O., 2022. Control of an AUV with completely unknown dynamics and multi-asymmetric input constraints via off-policy reinforcement learning. Neural Comput. Appl. 34, 5255–5265.

Shang, Y., Chen, B., Lin, C., 2018. Consensus tracking control for distributed nonlinear multiagent systems via adaptive neural backstepping approach. IEEE Trans. Syst. Man Cybern.: Syst. 50, 2436–2444.

Shen, C., Shi, Y., Buckham, B., 2018. Trajectory tracking control of an autonomous underwater vehicle using Lyapunov-based model predictive control. IEEE Trans. Ind. Electron. 65, 5796–5805. http://dx.doi.org/10.1109/TIE.2017.2779442.

Shojaei, K., 2022. Neural network feedback linearization target tracking control of underactuated autonomous underwater vehicles with a guaranteed performance. Ocean Eng. 258, 111827.

Sontag, E.D., 1998. Mathematical Control Theory: Deterministic Finite Dimensional Systems. Springer-Verlag, New York.

Wang, H., Chen, B., Liu, K., Liu, X., Lin, C., 2013. Adaptive neural tracking control for a class of nonstrict-feedback stochastic nonlinear systems with unknown backlash-like hysteresis. IEEE Trans. Neural Netw. Learn. Syst. 25, 947–958.

Wang, H., Chen, B., Liu, X., Liu, K., Lin, C., 2014. Adaptive neural tracking control for stochastic nonlinear strict-feedback systems with unknown input saturation. Inform. Sci. 269, 300–315.

Wang, J., Wang, C., Wei, Y., Zhang, C., 2019. Command filter based adaptive neural trajectory tracking control of an underactuated underwater vehicle in three-dimensional space. Ocean Eng. 180, 175–186.

Xu, R., Tang, G., Xie, D., Han, L., Huang, H., 2022. Neural network for 3d trajectory tracking control of a cmg-actuated underwater vehicle with input saturation. ISA Trans. 123, 152–167.

Yan, Z., Wang, M., Xu, J., 2019. Global adaptive neural network control of underactuated autonomous underwater vehicles with parametric modeling uncertainty. Asian J. Control 21, 1342–1354.

Yu, J., Fu, C., Liu, J., Ma, Y., 2023. Barrier Lyapunov function-based finite-time dynamic surface control for output-constrained nonstrict-feedback systems. J. Syst. Sci. Complex. 36, 524–539. http://dx.doi.org/10.1007/s11424-023-1330-x.

Yu, J., Shi, P., Lin, C., Member, S., Yu, H., 2020. Adaptive neural command filtering control for nonlinear MIMO systems with saturation input and unknown control direction. IEEE Trans. Cybern. 50, 2536–2545. http://dx.doi.org/10.1109/TCYB.2019.2901250.

Zhang, J., Xiang, X., Lapierre, L., Zhang, Q., Li, W., 2021. Approach-angle-based three-dimensional indirect adaptive fuzzy path following of under-actuated AUV with input saturation. Appl. Ocean Res. 107, 102486. http://dx.doi.org/10.1016/j.apor.2020.102486.

Zhang, J., Xiang, X., Zhang, Q., Li, W., 2020. Neural network-based adaptive trajectory tracking control of underactuated AUVs with unknown asymmetrical actuator saturation and unknown dynamics. Ocean Eng. 218, 108193.

Zhao, K., Song, Y., Ma, T., He, L., 2018. Prescribed performance control of uncertain euler–lagrange systems subject to full-state constraints. IEEE Trans. Neural Netw. Learn. Syst. 29, 3478–3489. http://dx.doi.org/10.1109/TNNLS.2017.2727223.

Zheng, X., Yang, X., 2020. Command filter and universal approximator based backstepping control design for strict-feedback nonlinear systems with uncertainty. IEEE Trans. Automat. Control 65, 1310–1317. http://dx.doi.org/10.1109/TAC.2019.2929067.

Zong, G., Sun, H., Nguang, S.K., 2021. Decentralized adaptive neuro-output feedback saturated control for INS and its application to AUV. IEEE Trans. Neural Netw. Learn. Syst. 32, 5492–5501.

Zuo, Z., Wang, C., 2014. Adaptive trajectory tracking control of output constrained multi-rotors systems. IET Control Theory Appl. 8, 1163–1174.